# STUDY ON INGAP/GAAS COLLECTOR-UP HBTS WITH THE GRAPHENE BASE FOR POWER-AMPLIFIER APPLICATIONS

**[1]WEI-MIN DU, [2]HSIEN-CHENG TSENG**

[1,2]Electronic Engineering, Department Tainan 71003, Taiwan Kun Shan University
E-mail: [1]fred.du.wei@gmail.com, [2]j41528@mail.ksu.edu.tw

**Abstract-** In this work, the characteristics of novel InGaP/GaAs collector-up heterojunction bipolar transistors with the graphene base and the nonuniform doped collector are demonstrated, and performances of the novel HBTs have been compared with the conventional InGaP/GaAs HBTs with various collector structures and thermal schemes. As compared to the conventional HBTs, the studied C-up HBTs exhibited better current-driving capability and higher RF efficiency. Note that the pnp device displayed greater thermal stability enhancement, which are distinct and reproducible, than the n-p-n device. The comparison results, based on pragmatic observations from the C-up HBTs without relatively large heat-dissipation configurations, should be very useful for the reliable and the cost-effective design as small-scale power amplifiers in the wideband CDMA (W-CDMA) system.

**Keywords**- Collector-Up, Graphene, Heterojunction Bipolar Transistors, Power Amplifiers, Thermal Stability.

## I. INTRODUCTION

POWER amplifiers (PAs) based on heterojunction bipolar transistors (HBTs) have been one of key technologies in providing resolutions for strict requirements on high efficiency and high-linearity of PAs in various wireless communication systems [1], [2]. Reliability and stability of the microwave PAs are important issues for them being used in high-data-rate transmission and internet access systems, such as a wideband code-division-multiple-access (W-CDMA) system [3]. High-performance PAs usually deliver precise control of power-transmitted levels, and most efficient use of power, i.e., thermal management. Because of their RF characteristics at low-bias voltages and their relatively high power-handling capability, InGaP/GaAs HBTs have been proven useful as the active component of linearized PAs in the wireless digital mobile communication. Additionally, to further expand the application of HBT-based PAs, small-scale devices and systems must be developed. In fact, the wafer-level miniaturization of PAs depends mainly on appropriate reliability and thermal management in HBT designs.

Compared with Si-Ge HBTs, GaAs-based devices are more sensitive to the failure mechanisms, such as self-heating and the breakdown effect. Firstly, the thermal conductivity of GaAs is much lower than that of Si and that makes the GaAs devices more prone to self-heating. Secondly, the current density used for GaAs HBTs is usually much higher than that used for Si-based transistors, and the collectors of GaAs HBTs are usually lightly doped. This will cause the breakdown voltage to drop radically as the collector current increases. At present, most of HBT-based PAs employing emitter-up (E-up) configuration, where the emitter layer is located on the surface, have been limited by serious thermal effects. In contrast, the collector-up (C-up) configuration in HBTs had been shown to ease the heat-dissipation dilemma [4], [5]. A number of research literatures proposed special thermal and power measures, such as ballast resistors [6], thermal shunts [7], and wide finger pitch [8] for multi-finger devices. However, HBTs with the aforementioned measures as the PA module are difficult to be integrated as highly compact power ICs. On the other hand, to provide high levels of efficiency and reliability at low levels of power consumption, the nonuniform collector design employed a thin high-doping collector layer [9] and the tunneling-collector structure incorporated a thin tunneling barrier at the base-collector junction had been reported [5].

In this article, we further expands our work on [10] by using the thermal-stability design implemented in multi-finger devices with the thin graphene base, and to achieve high-performance HBT-based PAs. We present novel InGaP/GaAs pnp and npn C-up HBTs without thermal-via holes [5], which are quite different from previously proposed transistors. The results showed that the thermal effects were effectively lessened compared to the published work, and the radio-frequency (RF) performance was promising.

## II. DEVICE STRUCTURE AND FABRICATION

Layer structures of standard InGaP/GaAs C-up npn and pnp HBTs, grown on two semi-insulating GaAs substrates, are outlined in Table 1. Device fabrication process consists of the following steps. Firstly, a non-alloyed WSi metal was laid down to provide the collector electrode and etching mask. The collector was then formed by reactive-ion etching (RIE). A small emitter layer was realized by boron-ion implantation. The collector and external base areas were defined by selective etching. At the same time, the external emitter was defined and the device was isolated. After removing the GaAs on the external

base by selective etching, the collector and emitter contacts were defined.

A simple selective etching technique is indispensable to the successful fabrication of devices. Separate metallizations were used to form nonalloyed contacts. Our device design employed the GaAs/InGaP material system applying disordered InGaP lattice-matched to GaAs with an indium composition of 0.5. The InGaP layer was selectively etched (using HCl) over GaAs layer, which made the device etching regular. Polymide was used to produce the interlayer dielectric to reduce the interconnect crossover parasitic capacitance and planarize the second metal process. After the front-side process was completed, the substrate was thinned down to a thickness of 100 μm.

## III. RESULTS AND DISCUSSION

### 3.1. DC Characterization

Fig. 1 shows the collector current ($I_c$)–collector-emitter voltage ($V_{ce}$) characteristics of one-finger C-up npn HBTs. In contrast to the $I_c$–$V_{ce}$ characteristics dotted lines) of the conventional InGaP/GaAs HBT, the $I_c$–$V_{ce}$ characteristics (solid lines) of the C-up HBT showed no obvious negative differential slope. The negative differential slope has been attributed to self-heating of the HBTs, in the case of a conventional GaAs HBT [11]. These results thus suggest that the novel base-graded structure plays a part in the effective heat radiation of the C-up HBT.

HBTs, as in all bipolar transistors, suffer from various feedback phenomena, which may cause thermal instability and device failure in certain operating conditions. The most well-known damaging effect is the “thermal runaway” caused by self-heating [12]. When a bipolar transistor is operated at high powers, the increased junction temperature causes the bandgap energy and consequently the junction built-in potential to drop. Therefore, the collector current increases. For our devices, the collector current is given by [13]

$$I_c = I_{S0} \cdot \exp\left\{ \frac{q}{k[T_A + (R_{th} \cdot I_c \cdot V_{CE})]} \cdot [V_{BE} - [(h_{fe}+1) \cdot R_e + R_b] \cdot I_b - E_g(T_j)] \right\} \quad (1)$$

where $I_{S0}$ is the collector saturation current, $T_A$ is the ambient temperature, $h_{fe}$ (= $I_c/I_b$) is the current gain, $R_e$ is the extrinsic emitter resistance, $R_b$ is the extrinsic base resistance, $I_b$ is the base current, and $E_g(T_j)$ represents energy gap at the junction temperature.

The voltage applied across the base-emitter junction can be expressed as

$$V_{BE} = V_{be} + I_b \bullet [(h_{fe} + 1) \bullet R_e + R_b] \quad (2)$$

By re-arranging the above equation and taking into account the expression for the $I_c$, the $V_{BE}$ can be derived as

$$V_{BE} = \left(\frac{k}{q}\right) \cdot [T_A + (R_{th} \cdot I_C \cdot V_{CE})] \cdot \ln\left(\frac{I_C}{I_{S0}}\right) + \left(\frac{I_C}{h_{fe}}\right) \cdot [(h_{fe}+1) \cdot R_e + R_b] + \left(\frac{1}{q}\right) \cdot E_g(T_j).$$

(3)

In the C-up HBTs, the thermal stability can be explained by the correlation between the collector current and the base-emitter voltage as base current increases under a certain collector-emitter voltage. Accordingly, the thermal instability in the HBTs occurs at the bias condition, where $\partial I_C/\partial V_{BE} \rightarrow \infty$ (i.e., $\partial V_{BE}/\partial I_C = 0$ at the regression point). As mentioned above, the $I_{C0}$ at the regression point can be obtained from the differential of (3) for the $I_C$ as follows:

$$\frac{\partial V_{BE}}{\partial I_C} = \left(\frac{k}{q}\right) \cdot \left\{ (R_{th} \cdot V_{CE}) \ln\left(\frac{I_{C0}}{I_{SO}}\right) + \frac{T_A}{I_{C0}} + R_{th} \cdot V_{CE} \right\} + \left(\frac{1}{h_{fe}}\right) \cdot \{(h_{fe}+1) \cdot R_e + R_b\} = 0. \quad (4)$$

The result of the effects discussed above may lead to device instability. If we plot the device I–V, based on the collector current versus base-emitter voltage relationship, as shown in Fig. 2, the I-V curve at certain collector-emitter bias will bend over at a critical base voltage. To make a comparison, if we plot the device I-V, based on the collector current versus collector-emitter voltage relationship, as shown in Fig. 3, for certain base-emitter bias, the curve will also bend over at certain critical voltage. When the device reaches the regression point, it becomes unstable because it can go into two paths, one with a high current and the other with a low current. In cases of multi-finger transistors, multiple solutions result and the currents of some fingers may run out of control. In accordance with observations of Figs. 2 and 3, the pnp C-up HBT clearly exhibited higher regression point than that of the conventional InGaP/GaAs HBT.

Subsequently, we investigated the influence of the device design on the thermal stability in our C-up HBTs. As depicted in Figs. 2 and 3, the C-up HBT with the tunneling collector exhibited good regression characteristics; but for our C-up HBTs, the pnp device exhibited better performance than the npn device. The increase in the regression point of the pnp device could be attributed to the n-type graded base. Here, we examine the influence on the regression characteristics, by using the theoretical analysis based on (4). It indicates that the expansion of the thermal stability in the C-up pnp HBT, with the graded InGaAs base, can be explained by the higher electron mobility resulting in low base resistance and higher emitter resistance.

### 3.2. RF Characterization

Table 2 presents the various collector structures compared in this paper. Nonuniform collector doping design is the principal nonlinear element in HBTs

[14]-[17]. In this study, a highly doped layer is combined with the low-doped collector. The highly doped region is required to accommodate the electric field induced by the collector–base voltage. This collector design rearranges the electric fields in the collector to delay the inception of the device instability, thus improving the current handling capability and linearity of the C-up HBT.

Advanced wireless communication, and primarily those for W-CDMA systems, requires PAs with a high power-added efficiency (PAE) and a low adjacent-channel-leakage power ratio (ACPR) over a wide range of output power levels (Pout). Fig. 4 shows the dependence of the PAE and the gain on input power that was carried out at 2.0 GHz. The PA design was fine-tuned to improve thermal and RF stability as well as gain and efficiency. Consequently, a high PAE of ~ 58% is achievable. Fig. 5 shows the adjacent-channel-leakage power ratio (ACPR) versus output power at 1.9 GHz. The ACPR of the C-up npn HBT, which is less than –42 dBc at 27 dBm for typical CDMA applications, was estimated to exceed that of the conventional InGaP/GaAs HBT.

## CONCLUSIONS

We have studied the DC/RF characteristics and thermal stability of the InGaP/GaAs C-up HBTs, with the graphene base and the nonuniformly doped collector, by comparing them to the advanced HBTs with relatively large heat-dissipation designs and the C-up HBTs with a thermal via. This work has developed a novel structure for the improvement of stability and reliability. As a result, the roles of emitter resistance and base resistance on thermal-stability of devices operated at high currents have been scrutinized through I-V analyses. For RF characterization, the C-up HBT PA exhibits high linearity with a high PAE of ~ 58% at 2.0 GHz and an ACPR of over –48 dBc.

Attributable to the higher emitter resistance and lower base resistance, which result in the reduction in thermal resistance, of the C-up pnp HBTs, we have achieved encouraging performances from the proposed device configurations. Noticeably, the innovative C-up HBT structures, which enhance the power-handling capability and thermal stability of the InGaP/GaAs HBTs, can be used as small-scale PAs for wireless communication applications.

## ACKNOWLEDGMENTS

The authors would like to thank technical support from the ITRI. This work is supported in part by the Ministry of Science and Technology (MOST) under Grant MOST 105-2221-E-168-023.

## REFERENCES

[1]J. D. Cressler, “Emerging SiGe HBT reliability issues for mixed-signal circuit applications,” IEEE Trans. Device Mater. Rel., vol.4, no.2, pp. 222-236, Jun. 2004.

[2]C. H. Lin, Y. K. Su, Y. Z. Juang, C. F. Chiu, S. J. Chang, J. F. Chen, and C. H. Tu, “The optimized geometry of the SiGe HBT power cell for 802.11 a WLAN applications,” IEEE Microw. Wireless Compon. Lett., vol.17, no.1, pp.49-51, 2007.

[3]G. Hau, T. B. Nishimura, and N. Iwata, “A highly efficient linearized wide-band CDMA handset power amplifier based on predistortion under various bias conditions,” IEEE Trans. Microw. Theory Tech., vol.49, pt.2, no.6, pp.1194-1202, Jun. 2001.

[4]L. I. Choi, A. Sibaja-Hernandez, R. Venegas, S. Van Huylenbroeck, and S. Decoutere, “SiGe HBTs with normal high-speed emitter-up and reverse low-power collector-up operation,” IEEE Trans. Electron Devices, vol.55, no.1, pp.358-364, Jan. 2008.

[5]H. C. Tseng, J. K. Li, and T. W. Chen, “Thermal stability enhancement of InGaP/GaAs collector-up HBTs,” IEEE Trans. Device Mater. Rel., vol. 11, no.3, pp. 387–390, Sep. 2011.

[6]G. B. Gao, M. S. Unlu, H. Morkoc, and D. L. Blackburn, “Emitter ballasting resistor design for the current handling capability of AlGaAs/GaAs power heterojunction bipolar transistors,” IEEE Trans. Electron Devices, vol.38, no.2, pp.185-196, Feb. 1991.

[7]M. C. Tu, H. Y. Ueng, and Y. C. Wang, “Performance of high-reliability and high-linearity InGaP/GaAs HBT PAs for wireless communication,” IEEE Trans. Electron Devices, vol.57, no.1, pp.188-194, Jan. 2010.

[8]D. Floriot, J. C. Jacquet, E. Chartier, J. M. Coupat, P. Eudeline, P. Auxemery, and H. Blanck, “Thermal management of power HBT in pulsed operating mode,” in Proc. 35th Eur. Microw. Conf., 2005, vol.3, pp.1487-1490.

[9]M. Iwamoto, T. S. Low, C. P. Hutchinson, J. B. Scott, A. Cognata, X. Qin, L. H. Camnitz, P. M. Asbeck, and D. C. D’Avanzo, “Influence of collector design on InGaP/GaAs HBT linearity,” in Proc. IEEE MTT-S Int. Microw. Symp. Dig., Boston, MA, 2000, pp.757-760.

[10]Y. X. Horng, M. Y. Hsu, and H. C. Tseng, “An efficient thermal-removal design of GaAs/InGaAs/InGaP HBT-based power amplifiers,” presented at the IEEE PES Asia-Pacific Power and Energy Engineering Conference (APPEEC), Kowloon, Hong Kong, Dec. 2014, Paper 0098.

[11]K. Uchida, H. Matsuura, T. Yakihara, S. Kobayashi, S. Oka, T. Fujita, and A. Miura, “A series of InGaP/InGaAs HBT oscillators up to D-band,” IEEE Trans. Microwave Theory Tech., vol. 49, no.5, pp.858-865, May 2001.

[12]Y. Zhu, J. K. Twynam, M. Yagura, M. Hasegawa, T. Hasegawa, Y. Eguchi, Y. Amano, E. Suematsu, K. Sakuno, N. Matsumoto, H. Sato, and N. Hashizume, “Self-heating effect compensation in HBTs and its analysis and simulation,” IEEE Trans. Electron Devices, vol.48, no.11, pp.2640-2646, Nov. 2001.

[13]R. P. Arnold and D. S. Zoroglu, “A quantitative study of emitter ballasting,” IEEE Trans. Electron Devices, vol.21, no.7, pp.385-391, Jul. 1974.

[14]C. M. Wang, H. T. Hsu, H. C. Shu, and Y. Hsin, “High linearity InGaP/GaAs power HBTs by collector design,” IEEE Electron Device Lett., vol.25, no.2, pp.58-60, Feb. 2004.

[15]Y. -J. Jeon, H. -W. Kim, M. -S. Kim, Y. -S. Ahn, J. -W. Kim, J. -Y. Choi, D. -C. Jung, and J. -H. Shin, “Improved HBT linearity with a post-distortion type collector linearizer,” IEEE Microw. Wireless Compon. Lett., vol.13, no.3, pp. 102-104, Mar. 2003.

[16]T. Niwa, T. Ishigaki, H. Shimawaki, and Y. Nashimoto, “A composite-collector InGaP/GaAs HBT with ruggedness for GSM power amplifiers,” in Proc. IEEE Microw. Symp., Philadelphia, PA, Jun. 2003, pp.711-714.

[17]M. Pfost, V. Kubrak, and P. Zwicknagl, “Optimization of the collector profile of InGaP/GaAs HBTs for increased robustness,” in Proc. GaAs IC Symp., Scottsdale, AZ, 2003, pp. 115-118.

[18]M. G. Adlerstein and J. M. Gering, “Current induced degradation in GaAs HBTs,” IEEE Trans. Electron Devices, vol. 47, no.2, pp. 434-439, Feb. 2000.

**Table 1:Layer Structures of Standard InGaP/GaAs Collector-Up HBTs**

| Layer | Material | Thickness (Å) | | Doping ($cm^{-3}$) | |
|---|---|---|---|---|---|
| | | npn | pnp | npn | pnp |
| Cap | In(0.5)Ga(0.5)As | 500 | 500 | n> $1\times10^{19}$ | p> $1\times10^{19}$ |
| Grading | GaAs-In(0.5)Ga(0.5)As | 500 | 500 | n> $1\times10^{19}$ | p> $1\times10^{19}$ |
| Collector | GaAs | 6000 | 4000 | n=$3\times10^{16}$ | p=$4\times10^{16}$ |
| Grading | In(0.1)Ga(0.9)As-GaAs | 200 | 200 | n=$4\times10^{16}$ | p=$4\times10^{16}$ |
| Graphene Base | InGaAs with Thin Graphene Layer | 700 | 700 | p=$3\times10^{19}$ | n=$3\times10^{19}$ |
| Spacer | GaAs | 50 | 50 | i | i |
| Emitter | In(0.5)Ga(0.5)P | 300 | 300 | n=$5\times10^{17}$ | p=$5\times10^{17}$ |
| Sub-emitter | GaAs | 6000 | 6000 | n=$5\times10^{18}$ | p=$5\times10^{18}$ |
| Etch-stop | In(0.5)Ga(0.5)P | 500 | 500 | n=$4\times10^{18}$ | p=$3\times10^{18}$ |
| Semi-Insulating GaAs Substrate | | | | | |

Table 2:Various Collector Layer Structures

| Collector | Thickness | Doping |
|---|---|---|
| *HBT 1* | | |
| uniform doped | 7000 Å | $1\times10^{17}$ $cm^{-3}$ |
| *HBT 2* | | |
| nonuniform doped | 4500 Å | $8\times10^{15}$ $cm^{-3}$ |
| three layers | 200 Å | $5\times10^{17}$ $cm^{-3}$ |
| | 2300 Å | $8\times10^{15}$ $cm^{-3}$ |
| *HBT 3* | | |
| uniform doped | 8000 Å | $3\times10^{16}$ $cm^{-3}$ |
| tunneling layer | 50 Å | $5\times10^{17}$ $cm^{-3}$ |
| *HBT 4* | | |
| nonuniform doped | 6000 Å | $3\times10^{16}$ $cm^{-3}$ |
| two layers | 200 Å | $1\times10^{16}$ $cm^{-3}$ |

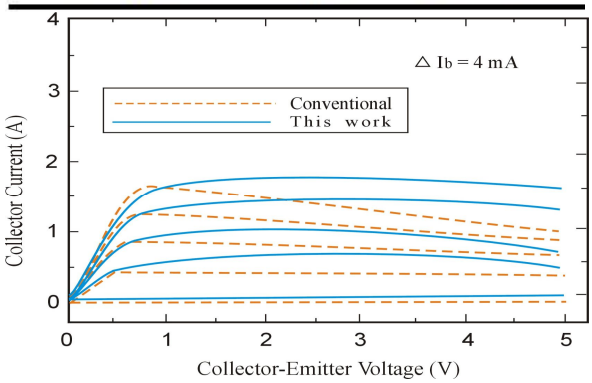


**Fig. 1. Current-voltage characteristics of the InGaP/ GaAs C-up HBTs with (solid lines) and without (dotted lines) the graphene base.**

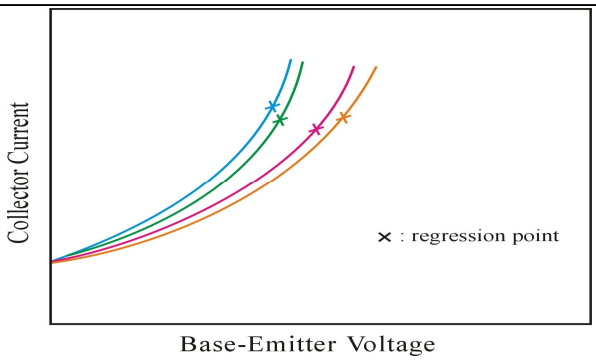


**Fig. 2. Dependence of collector current on the base-emitter voltage in the InGaP/GaAs HBTs (cross symbles indicate the regression point). (Blue line) The npn device with tunneling collector as proposed in [5]. (Green line) The npn device as propsed in this work. (Pink line) The npn device as proposed in [7]. (Orange line) The pnp device as proposed in this work.**

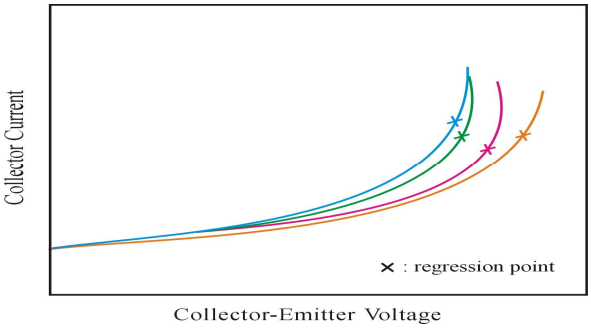


**Fig. 3. Dependence of the collector current on the collector-emitter voltage in the InGaP/GaAs HBTs (cross symbles indicate the regression point). (Blue line) The npn device with tunneling collector as proposed in [5]. (Green line) The npn device as propsed in this work. (Pink line) The npn device as proposed in [7]. (Orange line) The pnp device as proposed in this work.**

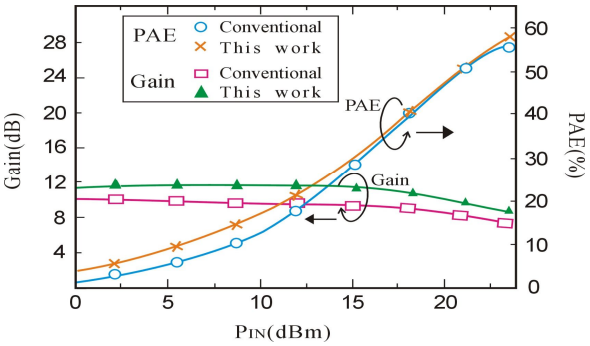


**Fig. 4. Dependence of the power-added efficiency (PAE) and the gain on input power for the devices (under identical vertical dimension) with (conventional) and without (this work) relatively large thermal designs.**

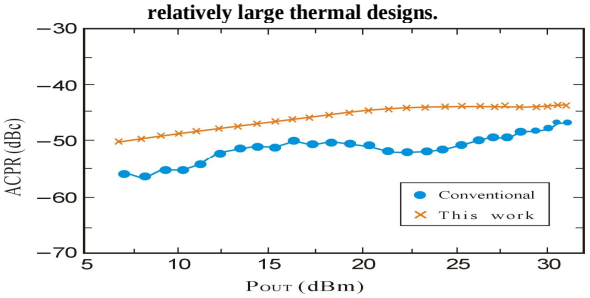


**Fig. 5. Adjacent-channel-leakage power ratio (ACPR) versus output power at 1.9 GHz for the devices (under identical vertical dimension) with (conventional) and without (this work) relatively large thermal designs.**